9212 *Biochemistry* **2009,** *48,* 9212–9220
DOI: 10.1021/bi900722p

BIOCHEMISTRY
including biophysical chemistry & molecular biology
Article

TonB Interacts with BtuF, the *Escherichia coli* Periplasmic Binding Protein for Cyanocobalamin[†]

Karron J. James,[‡] Mark A. Hancock,[§] Jean-Nicolas Gagnon,[‡] and James W. Coulton*[,‡]

[‡]*Department of Microbiology and Immunology,* [§]*Sheldon Biotechnology Centre, and McGill University, 3775 University Street, Montreal, Quebec, Canada H3A 2B4*

Received April 27, 2009; Revised Manuscript Received August 21, 2009

ABSTRACT: By its direct contact with outer membrane receptor BtuB, the cytoplasmic membrane transducer TonB delivers energy that mediates cyanocobalamin uptake in *Escherichia coli*. This activity has been generally proposed to be the role of TonB in cyanocobalamin uptake. We now report the discovery and characterization of interactions between TonB and periplasmic binding protein BtuF. Phage display experiments predicted interaction between TonB and BtuF, identifying potential binding residues on each protein. Dynamic light scattering experiments measured a complex of 55 kDa, consistent with a TonB−BtuF heterodimer. The hydrodynamic radius of the complex was unchanged in the presence of cyanocobalamin. Surface plasmon resonance measured TonB−BtuF interaction kinetics that were independent of cyanocobalamin and that deviated from a simple binding model. Binding isotherms from intrinsic fluorescence suggested a multifaceted interaction that was independent of cyanocobalamin. In addition, the presence of TonB did not abrogate subsequent binding of cyanocobalamin by BtuF. Taken together, these data support a previously proposed model wherein TonB serves as a scaffold to optimally position BtuF for initial binding of cyanocobalamin and for its subsequent release. These results substantiate a diverse role for TonB with its multiple protein−protein interactions in bacterial nutrient uptake systems.

TonB-dependent transport systems import a range of nutrients across the cell envelope of Gram-negative bacteria. These systems consist of a receptor located in the outer membrane (OM),[1] a binding protein located in the periplasm, and a cytoplasmic membrane- (CM-) associated ATP-binding cassette transporter. A central component of these systems is TonB, an elongated protein that is anchored in the CM and extends into the periplasm. Import of nutrients, including some that are essential for survival of bacteria, is severely reduced in the absence of TonB (*1*).

Escherichia coli TonB is a 25 kDa protein composed of three continuous and interconnected domains (*2*): N-terminal, residues 1−33; intermediate, residues 34−102; C-terminal, residues 103−239. Numerous reports (*3*−*6*) have demonstrated formation of complexes between TonB and OM receptors. X-ray crystallographic studies have illustrated interactions and identified residues within the C-terminal domain of TonB that make direct contact with OM receptors (*7*, *8*). The TonB−ExbB−ExbD CM protein complex is proposed (*9*−*11*) to harness energy of the protonmotive force and to transfer this energy to the OM receptor. Interaction of TonB with an OM receptor drives uptake of substrate across the OM.

The Btu system is used by *E. coli* for TonB-dependent import of vitamin B_{12}, also called cyanocobalamin (*12*). After its import across the OM receptor BtuB, cyanocobalamin is bound by periplasmic binding protein BtuF. ATP hydrolysis by CM-associated BtuD provides energy for uptake of cyanocobalamin through the CM permease BtuC. The crystal structure of BtuB in complex with the C-terminal domain of TonB (*8*) illustrated formation of an interstrand β-sheet between the Ton box of BtuB (residues 6−12) and a β-strand of TonB (residues 226−232). This complex represents interactions between BtuB and TonB after substrate binding to BtuB and perhaps during the transfer of energy from TonB to BtuB. The crystal structure of BtuF in complex with BtuCD (*13*) likely demonstrates their interaction after transport of cyanocobalamin across the CM. Although other reports (*12*, *14*, *15*) have provided evidence for these stages of the TonB-dependent uptake of cyanocobalamin, that is, at the OM and at the CM, events in the periplasm are not as well characterized.

Periplasmic binding protein BtuF is a bilobed 28 kDa protein. Its two globular domains are connected by a single rigid α-helix, characteristic of class III periplasmic binding proteins (*15*, *16*). Other class III periplasmic binding proteins include FhuD (cognate ligand: ferrichrome) (*17*), PhuT (heme) (*18*), PsaA (manganese) (*19*), ShuT (heme) (*18*), and TroA (zinc) (*20*). The N-terminal domain of BtuF extends from residues 1 to 106, and the C-terminal domain includes residues 130−244 of the mature protein. Cyanocobalamin is bound in a cleft between the globular domains making contact with residues in both domains.

[†]This work was supported by operating grants to J.W.C. from the Canadian Institutes of Health Research (CIHR). Sheldon Biotechnology Centre is supported by a Research Resource Grant from CIHR. Canada Foundation for Innovation provided infrastructure for surface plasmon resonance to the Montreal Integrated Genomics Group for Research on Infectious Pathogens. K.J.J. is a recipient of scholarships from the Organization of American States and from the Canadian Commonwealth Scholarships Program.

*To whom correspondence should be addressed: tel, (514) 398-3929; fax, (514) 398-7052; e-mail, james.coulton@mcgill.ca.

[1]Abbreviations: CM, cytoplasmic membrane; DLS, dynamic light scattering; EDTA, ethylenediaminetetraacetic acid; IPTG, isopropyl β-D-thiogalactopyranoside; M_r, relative molecular mass; MBP, maltose-binding protein; OM, outer membrane; PDB, Protein Data Bank; R_H, hydrodynamic radius; RU, resonance unit; SPR, surface plasmon resonance.

 Published on Web 08/26/2009

We previously characterized novel binding interactions between TonB and FhuD, periplasmic binding protein in the ferric hydroxamate uptake system (*21*). TonB and FhuD formed a 1:1 complex that was independent of the presence of hydroxamate siderophore. This led to the following question: Is the TonB−periplasmic binding protein interaction unique to FhuD or do other class III periplasmic binding proteins also interact with TonB? To explore this question, we investigated whether TonB interacts with BtuF, a binding protein that displays high structural homology to FhuD, yet transports an unrelated substrate. Our molecular and biophysical characterizations clearly demonstrate that TonB contacts BtuF, a new finding that substantiates a diverse role for TonB through its interaction with both OM receptors and periplasmic binding proteins.

EXPERIMENTAL PROCEDURES

Phage Libraries and Bacterial Strains. Combinatorial peptide M13 phage libraries, Ph.D.-12 and Ph.D.-C7C, were purchased from New England BioLabs (NEB). *E. coli* ER2738 (NEB) was used for phage propagation. Hexahistidine-tagged TonB residues 32−239 were expressed in *E. coli* ER2655 (*3*). *E. coli* ER2566/pCMK01 expresses TonB residues 32−239 and includes an introduced cysteine at its N terminus (*22*). The *btuF* gene cloned into pET24a was a gift from J. F. Hunt (*16*); this plasmid was expressed in *E. coli* BL21(DE3). Maltose binding protein (MBP) and Ton box peptide−MBP fusion were both cloned into pMal-pIII and expressed in *E. coli* NM522 (*23*).

Protein Expression and Purification. TonB was expressed and purified by immobilized metal affinity chromatography and ion-exchange chromatography as previously described (*24*). For BtuF, bacteria were grown in Luria−Bertani broth, and BtuF was induced during midlogarithmic phase with 0.05 mM IPTG for 3 h at 30 °C. Harvested cells were resuspended in 50 mM monobasic sodium phosphate (pH 7.1), 200 mM sodium chloride, and 10 mM imidazole and lysed at 16000 psi during two cycles through an Emulsiflex-C5 homogenizer (Avestin). Clarified cell extract was affinity-purified on Ni^{2+}-NTA Superflow resin (Qiagen) followed by size exclusion chromatography on Superdex 75 (GE Healthcare Bio-Sciences). MBP and Ton box−MBP were expressed and purified as previously described (*23*). Purities of TonB and BtuF and of MBP variants were assessed by SDS−PAGE (12% polyacrylamide gels; 750 ng/lane) under reducing (5% (v/v) 2-mercaptoethanol) and nonreducing conditions followed by silver staining or by immunoblotting using anti-6×His monoclonal antibodies (Clontech). Protein concentrations were determined using Bradford assay (Bio-Rad).

Phage Display. To predict interactions between TonB and BtuF, affinity selection using BtuF as target was performed as previously described (*24*) using the Ph.D.-12 and the Ph.D.-C7C phage libraries (NEB). After two or three rounds of panning, DNA from phage clones was purified using the QIAprep 96 M13 kit (Qiagen) and sequenced at McGill University and Génome Québec Innovation Centre. Sequences of affinity-selected peptides were analyzed using the MATCH program in the REceptor LIgand Contacts (RELIC) bioinformatics suite (*25*) and MatchScan, its derivative bioinformatics program (P. D. Pawelek, unpublished; ref *21*).

Dynamic Light Scattering. Prior to dynamic light scattering (DLS) assays, all protein samples were dialyzed at 4 °C against 100 mM monobasic sodium phosphate (pH 7.1) containing 150 mM sodium chloride. Immediately prior to each assay, samples were centrifuged at 13000*g* for 15 min at 20 °C, and the supernatant was introduced into a 12 μL quartz cuvette for measurements. Experiments were performed as previously described (*21*). Individual proteins were assayed at 5 μM. TonB plus BtuF (2.5 μM each) was combined 30 min prior to each assay. BtuF alone and TonB plus BtuF were assayed in the absence and presence of cyanocobalamin (Sigma). As a positive control, a peptide (EDTITVTAA) representing residues 6−14 of OM receptor FhuA was expressed and purified as a fusion to MBP (*23*). This region of FhuA known as the Ton box has been previously (*7*, *23*, *26*) shown to interact with TonB. As a negative control, MBP was used. For each sample, 500 scans were recorded using a DynaPro E-50-830 instrument (Protein Solutions, Charlottesville, VA) with an averaging time of 10 s per measurement. Readings were recorded by Dynamics version 6.3.18 software. Three independent measurements were made for each sample using three different preparations of TonB and BtuF. Data used to compute the autocorrelation functions had baselines ≤1.01 and sum of squares ≤250.

Autocorrelation coefficients for each data set were imported into SEDFIT (*27*) version 11.3 for analysis using the Noninteracting Discrete Species model. Solvent density and viscosity were calculated using SEDNTERP version 1.09 (*28*). Sedimentation coefficients for TonB and MBP were obtained from the literature (*3*, *29*) whereas that for BtuF (2.12 *s*) was determined by analytical ultracentrifugation (K. J. James, C. Ng-Thow-Hing, and P. Schuck, unpublished data). SEDNTERP was used to standardize the sedimentation coefficients to $s_{20,w}$ values that were then constrained during analyses. A sedimentation coefficient for TonB in complex with FhuD was previously determined by analytical ultracentrifugation (*21*). This value was used as an initial prediction during Noninteracting Discrete Species model analyses of TonB plus BtuF data but was not constrained. Molecular mass predictions for each sample combination were refined by nonlinear least-squares regression analyses. In addition to the proteins being analyzed, size distribution histograms in the Dynamics program indicated the presence of smaller (< 1 nm) and larger (> 1000 nm) molecular mass species. Their presence was taken into account during data analyses using the SEDFIT Noninteracting Discrete Species model. The Continuous I(Rh)-Distribution model in SEDFIT was used to determine the hydrodynamic radius (R_H) of individual proteins and of protein complexes.

Surface Plasmon Resonance. Real-time binding of BtuF to TonB was characterized using Biacore 2000/3000 instrumentation (GE Healthcare Bio-Sciences AB, Uppsala, Sweden). Experiments were performed on research-grade CM4 sensor chips at 25 °C using filtered (0.2 μm) and degassed HBS-ET running buffer (50 mM HEPES (pH 7.4), 150 mM sodium chloride, 3 mM EDTA, 0.05% Tween 20 (Calbiochem)). TonB (3 μg/mL in 10 mM sodium acetate (pH 5.5)) was thiol-coupled to desired densities, and corresponding reference surfaces were prepared in the absence of TonB. BtuF was injected at 30 μL/min over the prepared surfaces for 300 s followed by injection of HBS-ET for 600 s. For all binding assays conducted in the presence of substrate, a 10-fold molar excess of cyanocobalamin was added to BtuF followed by incubation for 30 min at room temperature. As a negative control, MBP, periplasmic binding protein of a TonB-independent uptake family, was injected over reference and over TonB-immobilized surfaces. At the end of each titration series, surfaces were regenerated using HBS-ET containing

500 mM sodium chloride, 5 mM sodium hydroxide, and 0.05% Empigen. Equilibrium amounts of BtuF bound (Req) were determined by averaging steady-state plateaus for each concentration injected. Data were fit by nonlinear least-squares regression using SigmaPlot according to the four-parameter logistic equation:

$$y = A+((B-A)/(1+10^{(x-\log C_{50})(D)})) \quad (1)$$

where A represents the minimum signal response, B represents the maximum signal response, C_{50} represents the concentration of titrant that produces 50% of the maximum signal response, and D represents the slope factor. Scatchard analyses were performed by plotting the ratio of bound BtuF:free BtuF against the amount of bound BtuF.

Fluorescence Spectroscopy. All samples were dialyzed extensively against 100 mM sodium phosphate (pH 7.1) containing 150 mM sodium chloride and centrifuged at 12000*g* for 10 min prior to each steady-state fluorescence assay. Fluorescence measurements were conducted at 20 °C using a Varian Cary Eclipse fluorescence spectrophotometer. Excitation and emission slit widths were set to 5 nm. For titration assays, samples were excited at 295 nm, and fluorescence emissions were recorded at 320 nm. Triplicate emission spectra were recorded from 300 to 400 nm at a scan rate of 60 nm/min. BtuF or BtuF plus cyanocobalamin (10-fold molar excess) was maintained at 0.5 μM for titrations of TonB up to 5-fold molar excess; 0.5 μM BtuF was included with TonB titrant to eliminate dilution effects (*30*). After each TonB addition, solutions in the quartz cuvette were mixed and equilibrated for 5 min before triplicate readings. To ensure that readings after this incubation period were representative of the true end point of our assays, we measured fluorescence emissions of BtuF upon addition of a selected concentration of TonB after 2, 5, 10, 15, 20, 25, and 30 min. Complementary assays were performed in the identical manner to monitor changes in TonB fluorescence using BtuF as titrant. Readings collected from three independent protein preparations were corrected for fluorescence contributions by buffer and by titrant. Changes in fluorescence were calculated as percentages of the initial intensity value. Experimental data were fit by nonlinear least-squares regression using SigmaPlot according to the four-parameter logistic equation (eq 1).

RESULTS

Prediction of Binding Interface by Phage Display. Purity of BtuF preparations used for phage panning experiments was >95% as assessed by SDS−PAGE followed by silver staining (Figure S1) and by immunoblotting. From BtuF-targeted assays, 120 unique peptides were affinity-selected from the Ph.D.-12 library, and 81 unique peptides were affinity-selected from the Ph.D.-C7C library. To predict whether TonB interacts with BtuF, pairwise alignments were performed between each affinity-selected peptide and the amino acid sequence of TonB. Three consensus regions on TonB were identified as potential BtuF-binding interfaces: region I, residues 51−62 within the intermediate domain; region II, residues 116−139 within the C-terminal domain; region III, residues 155−163 within the C-terminal domain (Tables 1 and 2, Figure 1). Region III is depicted (Figure 2) on a surface representation of the NMR structure of TonB (*2*).

From complementary phage panning experiments in which TonB was used as the target, we previously isolated 240 unique affinity-selected peptides (*21*). Pairwise alignments of each peptide to the amino acid sequence of BtuF identified three consensus regions (Tables 3 and 4, Figures 3 and 4) on BtuF within which TonB is predicted to bind; region I, residues 6−17 and 25−37 within the N-terminal domain; region II, residues 175−181 within the C-terminal domain; region III, residues 213−219 and 230−233 within the C-terminal domain of BtuF. All predicted TonB-binding residues occur on the same face of BtuF to which cyanocobalamin binds. Four residues within region I, Ser8, Pro9, Ala10, and Tyr28, and one residue within region III, Ser219, make direct contact with cyanocobalamin. Coincidence of these predicted TonB-binding residues with cyanocobalamin-binding residues suggests that TonB may bind BtuF that is substrate-free. Sequence comparisons with other class III periplasmic binding proteins from Gram-negative bacteria (Figure 5) show that predicted TonB-binding residues occur within regions of conserved secondary structure. A number of predicted binding residues are highly conserved. Some of these residues in the N-terminal domain of BtuF overlap with residues of FhuD that were predicted to bind TonB (*21*).

As a positive control, we performed pairwise alignments between the 201 BtuF affinity-selected peptides and the amino acid sequence of BtuC whose interaction with BtuF has already been demonstrated (*13*, *31*). The peptides clustered at four regions on the periplasmic face of BtuC (Supporting Information Tables S1 and S2, Figure S2) and include matches with Arg56 and Arg59,

Table 1: BtuF Affinity-Selected Ph.D.-12 Peptides Mapped to TonB

peptide[a]	region: domain	first residue of scoring window	peptide MATCH score[b]	scoring window[c]
RKK**TPA**S**RRP**MR	I: intermediate	51	14	7
DLKPPIPS**QS**GP	I: intermediate	54	18	9
SPPYTYL**PQK**V**Q**	I: intermediate	58	15	5
HMGAD**PL**QK**RPS**	II: C-terminal	116	14	6
DLFAR**RPAS**SDW	II: C-terminal	119	15	5
HFQMFH**RPS**G**P**Q	II: C-terminal	120	13	5
SHQMA**W**P**LEATS**	II: C-terminal	122	14	7
WHWTNWGK**TSPA**	II: C-terminal	127	13	5
QHQHV**NTL**P**ERP**	II: C-terminal	127	14	6
HNWLYY**L**RT**STA**	II: C-terminal	133	16	6
HWRLPL**LTS**LM**A**	II: C-terminal	133	14	6
N**LTSL**TQG**SA**ML	II: C-terminal	133	15	5

[a]Residues in bold represent exact matches, within the scoring window indicated, to the amino acid sequence of TonB. [b]Modified BLOSUM62 matrix (*25*) used for scoring. [c]Represents the number of residues within the scoring window.

Table 2: BtuF Affinity-Selected Ph.D.-C7C Peptides Mapped to TonB[a]

peptide	region: domain	first residue of scoring window	peptide MATCH score	scoring window
H**PTPTDI**	I: intermediate	51	13	5
VHPYESH	II: C-terminal	114	14	6
DSPLSNL	II: C-terminal	123	12	5
H**LTS**MQM	II: C-terminal	132	12	4
HLQ**TSSS**	II: C-terminal	134	13	4
WTPSPAT	II: C-terminal	134	14	6
Y**STA**VRE	II: C-terminal	136	12	4
TM**RAVSA**	III: C-terminal	154	13	4
MA**SLSRS**	III: C-terminal	155	14	5
ALKTNQP	III: C-terminal	155	19	7
SHTQPYL	III: C-terminal	157	12	5

[a]See legend for Table 1.

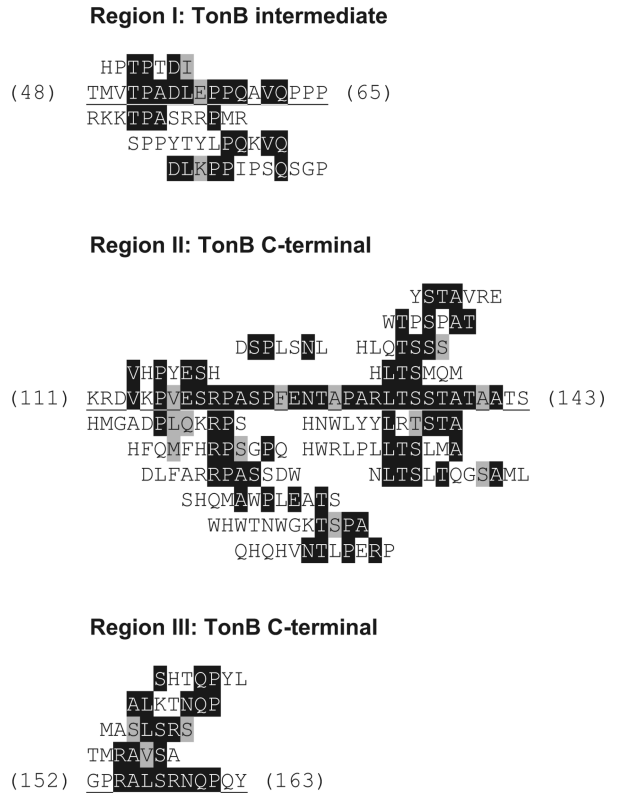

FIGURE 1: BtuF affinity-selected peptides aligned with the amino acid sequence of TonB. TonB sequences are underlined, and boundaries are indicated in parentheses. Regions I, II, and III identified by pairwise alignments of the TonB sequence to each affinity-selected peptide from the Ph.D.-C7C and Ph.D.-12 libraries in panning assays using purified BtuF. Unique 7 amino acid and 12 amino acid affinity-selected peptides are shown above and below TonB sequences, respectively. Exact sequence matches are highlighted in black; conservative matches are highlighted in gray.

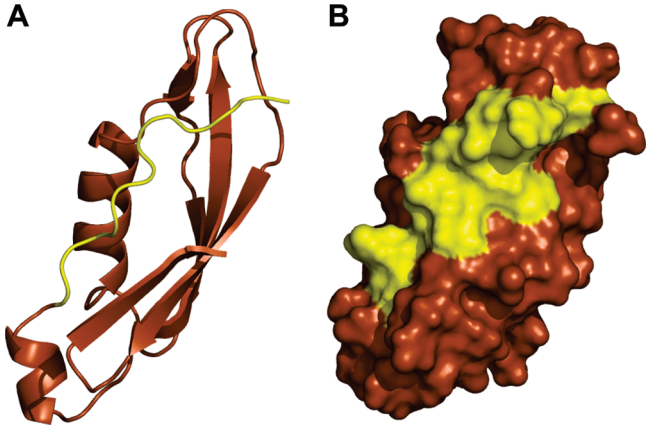

FIGURE 2: Predicted BtuF-binding site on the C-terminal domain of TonB. TonB region III (yellow), shown in Figure 1, identified by alignment of BtuF affinity-selected peptides to the amino acid sequence of TonB. (A) Ribbon and (B) surface representations, respectively, of the NMR structure of TonB (brown; PDB code 1XX3).

predicted (*15*) and confirmed (*13*) to interact with BtuF. Notably, alignment of our BtuF affinity-selected peptides to the primary sequence of the OM receptor BtuB did not produce significant matches, in contrast with matches for TonB and for BtuC.

Interaction of TonB with BtuF by DLS. DLS experiments were performed to determine if TonB and BtuF form a complex

Table 3: TonB Affinity-Selected Ph.D.-12 Peptides Mapped to BtuF

peptide[a]	region: domain	first residue of scoring window	peptide MATCH score[b]	scoring window[c]
SPAPTNNYTYRL	I: N-terminal	8	15	5
TDIVAHTSLQVR	I: N-terminal	10	13	5
TSRHHHTHLAMQ	I: N-terminal	11	13	5
TELSKAGHESYP	I: N-terminal	12	16	6
SSYARTLPHTYK	I: N-terminal	26	13	4
SYSNYQHHLPPA	I: N-terminal	27	17	5
GTPPMS**PLVSRV**	II: C-terminal	175	15	5
VSRHQSWHPHDL	II: C-terminal	177	16	5
GTP**PMSPLVSRV**	III: C-terminal	213	16	7
SHAL**PLTWSTAA**	III: C-terminal	214	13	5
KIWPPRMF**PLTS**	III: C-terminal	214	17	6
N**IIIGAHTTPTH**	III: C-terminal	229	13	5

[a]Residues in bold represent exact matches to the amino acid sequence of BtuF. [b]Modified BLOSUM62 matrix (*25*) used for scoring. [c]Represents the number of residues within the scoring window.

Table 4: TonB Affinity-Selected Ph.D.-C7C Peptides Mapped to BtuF[a]

peptide	region: domain	first residue of scoring window	peptide MATCH score	scoring window
LTR**SPAA**	I: N-terminal	5	16	6
TLSPKLH	I: N-terminal	6	15	5
ANV**SPAK**	I: N-terminal	7	13	5
ELN**VSSF**	I: N-terminal	25	13	5
QVSSHNT	I: N-terminal	25	14	5
RSTYSSE	I: N-terminal	26	13	5
NPIF**PQV**	II: C-terminal	174	13	4
QRLP**PLT**	III: C-terminal	214	12	5
SQV**PLKS**	III: C-terminal	215	12	5
IPRTNHQ	III: C-terminal	215	12	5
TK**PLTQ**Q	III: C-terminal	216	12	4
ILAASSA	III: C-terminal	230	16	5
LAALKST	III: C-terminal	231	12	5

[a]See legend for Table 3.

in solution. Purity of BtuF, TonB (Supporting Information Figure S1), and MBP preparations was >95% as assessed by SDS−PAGE followed by silver staining or by immunoblotting. Individual protein samples and combinations exhibited less than 18% polydispersity, as measured by Dynamics software, indicating low- to medium-polydisperse protein preparations. Relative molecular mass (M_r) data were all similar to theoretical predictions (Table 5) and to previously reported (*3*, *12*, *21*) values. Significantly, our M_r data indicate that TonB forms a complex with BtuF in solution both in the absence and in the presence of cyanocobalamin. We conclude that complexes measured at ~55 kDa represented TonB−BtuF heterodimers, consistent with a 1:1 binding stoichiometry. All root-mean-square deviation values derived from SEDFIT analyses were optimal, below 0.008 (Table 5). The relatively low abundance of complex, 34% or 41%, indicated the presence of incomplete factorials comprised of noncomplexed TonB and BtuF. Parameters for BtuF alone or TonB alone were included in noninteracting discrete species analyses, along with expected parameters for a TonB−BtuF complex. The outcomes revealed that up to 49% of the sample concentration during the course of an experiment consisted of noncomplexed proteins (data not shown). Nevertheless, TonB−BtuF complexes were resolved in all cases.

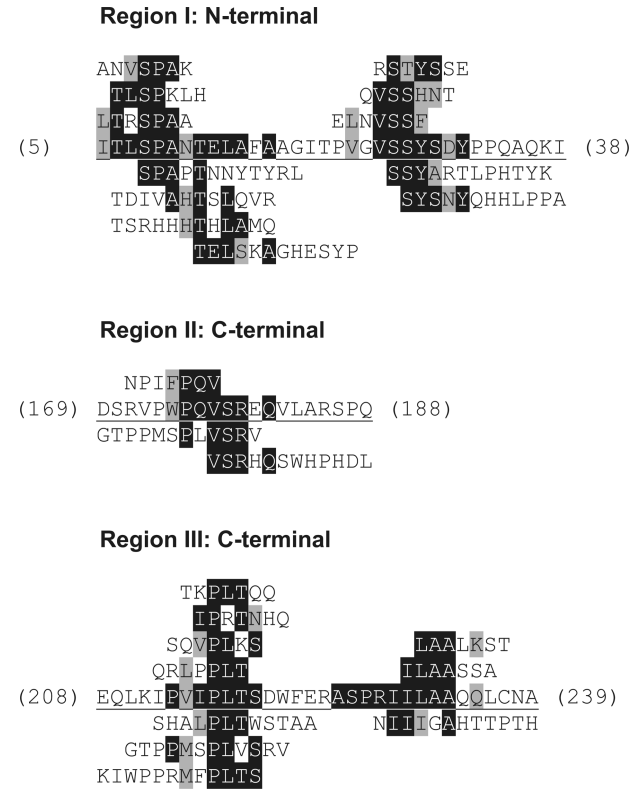

FIGURE 3: TonB affinity-selected peptides aligned with the amino acid sequence of BtuF. BtuF sequences are underlined, and boundaries are indicated in parentheses. Regions I, II, and III identified by pairwise alignments of the BtuF sequence to each affinity-selected peptide from the Ph.D.-C7C and Ph.D.-12 libraries in panning assays using purified TonB. Unique 7 amino acid and 12 amino acid affinity-selected peptides are shown above and below the BtuF sequences, respectively. Exact sequence matches are highlighted in black; conservative matches are highlighted in gray.

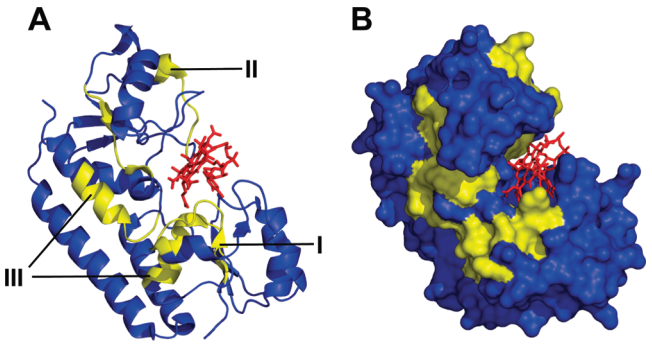

FIGURE 4: Predicted TonB-binding sites on BtuF. I, II, and III (yellow) correspond to BtuF regions, indicated in Figure 2, identified by alignment of TonB affinity-selected peptides to the amino acid sequence of BtuF. (A) Ribbon and (B) surface representations, respectively, of the X-ray structure of BtuF (blue; PDB code 1N4A). Stick representation of cyanocobalamin is shown in red.

R_H measurements of 3.58 nm (Table 5) provide strong evidence for TonB−BtuF complexation in solution when this value is compared to R_H values for TonB alone and for BtuF alone. Further, comparison with the R_H of TonB, 4.20 nm (Table 5), indicates that the interaction was accompanied by conformational change in TonB. Although our data for BtuF consistently indicate a slight contraction of its R_H in the presence of cyanocobalamin compared to the R_H of BtuF in the absence of cyanocobalamin (2.82 and 3.05 nm, respectively; Table 5), BtuF with bound cyanocobalamin formed complexes with TonB that were identical in size to complexes formed with apo-BtuF. BtuF R_H are commensurate with its more globular nature (*15*, *16*) compared to TonB that is postulated to have an elongated structure (*32*).

To validate the predicted stoichiometry of TonB−BtuF interactions, DLS experiments were also performed using excess TonB or excess BtuF. In each case, only outcomes for a 1:1 complex were observed; there was no evidence for participation of more than one component in complex with the other species. As a positive control, TonB was incubated with equimolar amounts of a Ton box−MBP fusion protein. Our analyses detected complex formation between TonB and this region of OM receptor FhuA (Table 5) as previously demonstrated by molecular genetics (*23*), biochemical (*26*), and crystallographic studies (*7*). As a negative control, we performed experiments using TonB and MBP combined in equimolar amounts. Only single species could be modeled in our SEDFIT analyses; no TonB−MBP complex was detected.

Interaction of TonB with BtuF by SPR. We investigated real-time binding of BtuF to immobilized TonB by SPR. Low-density TonB surfaces, ~200 resonance units (RU), were thiol-coupled. BtuF titrations, 0−2 μM, displayed specific, concentration-dependent, saturable binding to TonB (Figure 6). Injections of BtuF that had been preincubated with cyanocobalamin produced similar profiles as apo-BtuF, suggesting that BtuF interacts with TonB in a cyanocobalamin-independent manner (Figure 6). Global analyses of the titration series with a simple binding model yielded poor fits. Nonlinear least-squares regression of plots of Req versus BtuF concentration produced S-shaped profiles with C_{50} values of 0.55 ± 0.12 and 0.60 ± 0.10 μM for binding in the absence and presence of cyanocobalamin, respectively (Figure 6C,D). The goodness of fit of the data to the model, determined by the correlation coefficient, was 97% and 98%, respectively. Scatchard transformations (insets in Figure 6C,D) revealed convex profiles, further evidence for a more complex binding mechanism. As a negative control, injection of 500 nM MBP yielded little or no specific binding (< 10 RU) to TonB surfaces.

Interaction of TonB with BtuF by Fluorescence Spectroscopy. To further our interaction analyses, we investigated TonB−BtuF binding by intrinsic tryptophan fluorescence spectroscopy. Plots of fluorescence emission over time that were used to validate readings for our steady-state experiments produced a horizontal line; readings taken after a 5 min incubation period were representative of the assay end point. Titration of TonB resulted in augmentation of BtuF fluorescence emissions by 60% (Figure 7A) accompanied by a 7 nm blue shift in the emission wavelength (data not shown). Nonlinear least-squares regression analyses of the S-shaped binding isotherms produced a C_{50} of 0.50 ± 0.02 μM with a correlation coefficient of 99%. Addition of cyanocobalamin to BtuF produced marked (80%) quenching of BtuF fluorescence (data not shown). Titration of TonB into BtuF plus cyanocobalamin resulted in augmentation of BtuF fluorescence emissions by 71% and produced similar S-shaped binding isotherms (Figure 7B). Analyses revealed a C_{50} of 0.57 ± 0.01 μM with a correlation coefficient of 99%. To thoroughly investigate their binding mechanism, we reversed the order with BtuF as the titrant; similar S-shaped profiles and C_{50} values were obtained (data not shown). Addition of cyanocobalamin to a solution containing TonB and BtuF produced fluorescence spectra showing marked quenching of fluorescence emissions similar to those

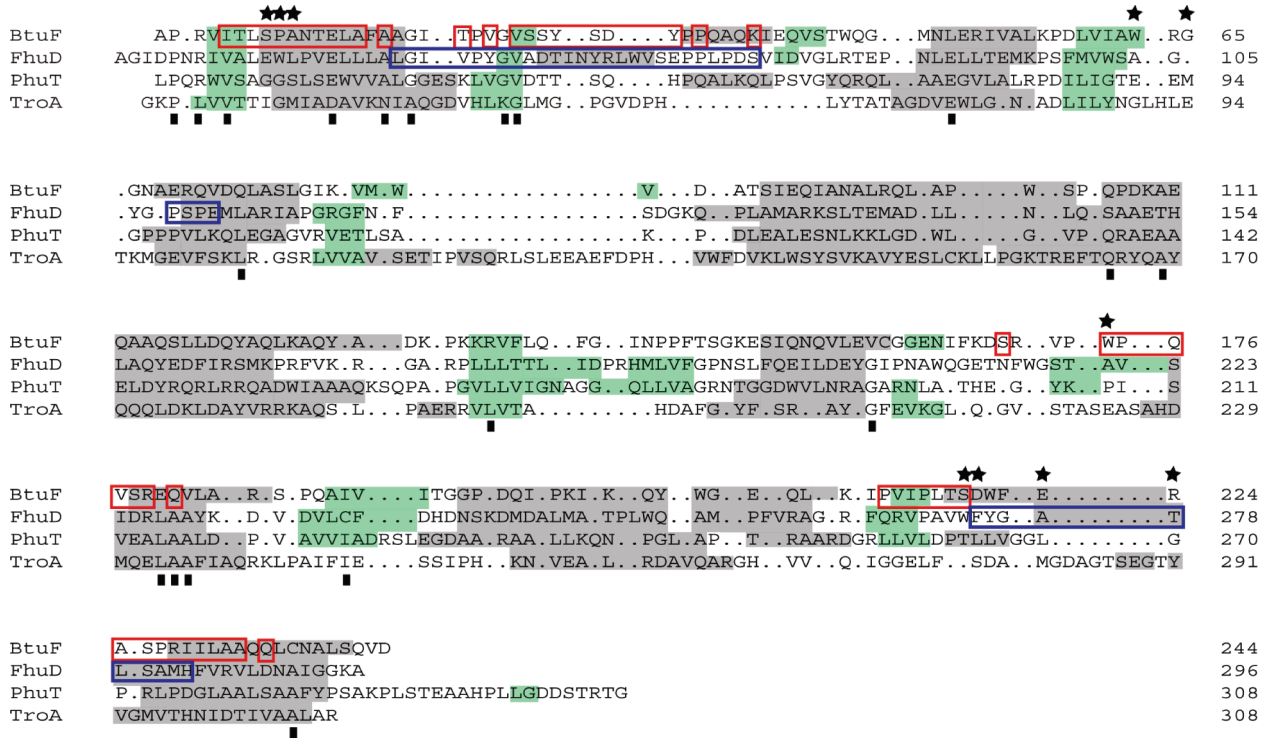

FIGURE 5: Structure-based sequence alignment of *E. coli* BtuF with other class III periplasmic binding proteins, FhuD (*E. coli*), PhuT (*P. aeruginosa*), and TroA (*T. pallidum*). Alignments were performed using STRAP (http://www.charite.de/bioinf/strap/) and PDB codes 1N4A, 1EFD, 2R79, and 1TOA. Conserved regions of α-helices are colored green, and *β*-strands are colored gray. Predicted TonB-binding residues on BtuF and on FhuD are indicated in red and blue boxes, respectively. BtuF residues that bind cyanocobalamin are indicated by solid stars. Conserved residues are identified by solid rectangles.

Table 5: DLS Analyses of TonB and BtuF

protein[a]	predicted M_r[b]	obsd M_r[c]	concn[d] (%)	rmsd[e]	R_H (nm)[f]	rmsd[g]
TonB	25111	24770	71	0.00265	4.20	0.00202
BtuF	28016	26822	87	0.00233	3.05	0.00195
BtuF + Cbl	29731	26228	71	0.00268	2.82	0.00406
TonB + BtuF	53127	55316	34	0.00344	3.58	0.00284
TonB + BtuF + Cbl	54482	58691	41	0.00607	3.58	0.00265
Ton box − MBP	41609	40902	70	0.00224	3.58	0.00368
TonB + Ton box − MBP	66720	64996	40	0.00079	3.88	0.00259
MBP	40700	39243	73	0.00599	2.80	0.00214
TonB + MBP	65000	22679	51	0.00796	na	na
		43631	48			

[a]Protein combinations mixed in 1:1 molar ratios; Cbl (cyanocobalamin) added in 10-fold molar excess of BtuF. [b]M_r, relative molecular mass in daltons, predictions based on amino acid sequence of protein constructs used. [c]M_r observed after minimization of rmsd in noninteractiong discrete species analysis. [d]Relative abundance of protein(s) in a sample as determined by SEDFIT. Components larger than 1000 kDa represented less than 10% of each sample whereas small molecular mass species accounted for the difference. [e]Minimized root-mean-square deviation in noninteracting discrete species analysis. [f]Determined using continuous I(Rh)-distribution model. na, not applicable. [g]Minimized rmsd of R_H measurements.

observed upon addition of cyanocobalamin to BtuF alone (data not shown). This outcome suggests that the presence of TonB did not abrogate binding of cyanocobalamin to BtuF.

DISCUSSION

Uptake of cyanocobalamin by the Btu family of proteins in *E. coli* is dependent upon TonB. Traditionally, the role of TonB, through its interactions with OM receptors, was thought to be that of energy transduction to facilitate active uptake of substrate into the periplasm. More recently, we demonstrated (*21*) that TonB interacts with the ferric hydroxamate periplasmic binding protein FhuD. The present study sought to determine whether this phenomenon was specific to ferric hydroxamate uptake or whether TonB also interacts with other periplasmic binding proteins in TonB-dependent transport systems. We now report that TonB interacts with BtuF. This interaction occurred with a stoichiometry of 1:1 and was independent of cyanocobalamin as was observed for FhuD and its substrate. We previously used phage display technology to predict binding interfaces for TonB−FhuA interactions (*23*) and for TonB−FhuD interactions (*21*). The TonB−FhuA predictions were confirmed by our cocrystal structure (*7*). In the present work, we again exploited phage display to predict interacting residues on TonB and on BtuF. Strikingly, TonB region II that is predicted to bind BtuF (Figure 1) is coincident with a region identified in the experiments using FhuD; residues 116−139 on TonB were identified from BtuF-targeted experiments, and residues 122−133 were identified

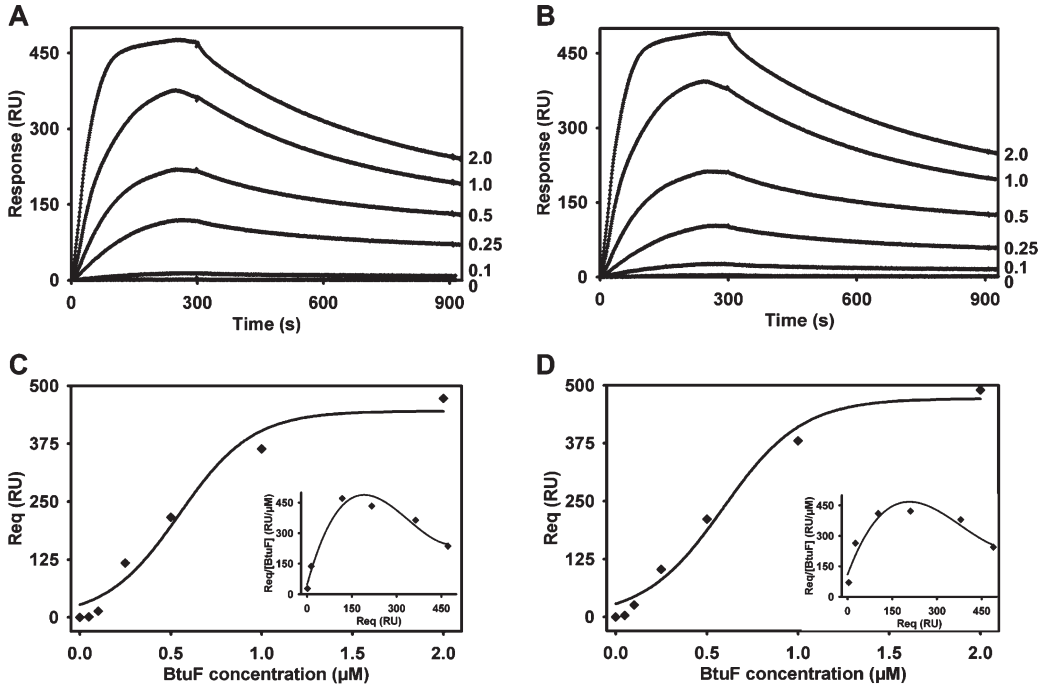

FIGURE 6: Real-time binding of BtuF to TonB. BtuF in the (A) absence and (B) presence of cyanocobalamin (10-fold molar excess) was injected over thiol-immobilized TonB. Injected BtuF concentrations, in μM, are shown on the right of each sensorgram. Sensorgrams were transformed into plots of plateau amounts of bound versus free (C) BtuF and (D) BtuF plus cyanocobalamin for steady-state analyses of their binding to TonB. Nonlinear least-squares regression produced C_{50} values of 0.55 $\pm$ 0.12 and 0.60 $\pm$ 0.10 μM, respectively. Insets correspond to Scatchard transformations of the data.

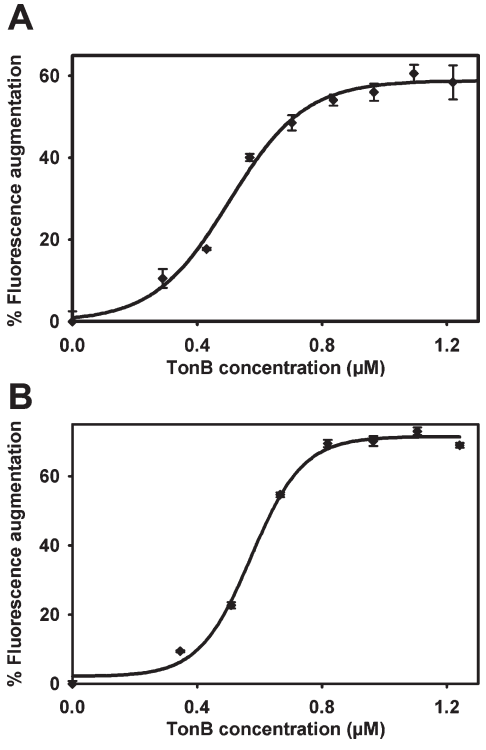

FIGURE 7: Solution-phase binding of TonB to BtuF and to BtuF plus cyanocobalamin. Steady-state increase in tryptophan fluorescence of (A) BtuF (0.5 μM) and (B) BtuF plus cyanocobalamin upon titration of TonB (0−1.56 μM). Solid lines represent fits of data (solid diamonds) $\pm$ standard errors to a four-parameter logistic model. Nonlinear least-squares regression produced C_{50} values of 0.50 $\pm$ 0.02 and 0.57 $\pm$ 0.01 μM for assays without and with cyanocobalamin, respectively. Assays were performed in triplicate and corrected for buffer and TonB contributions to fluorescence intensity. Data are representative of four independent assays.

from FhuD-targeted experiments. These residues, located in the C-terminal domain, are thought to be flexible; they were not resolved either in the crystal (*7*, *8*, *33*−*35*) or in the NMR (*2*) structures of TonB. Regions I and III on TonB are proximal to similar regions predicted to bind FhuD (*21*). The independent phage display outcomes and their convergence with outcomes from FhuD-targeted experiments further establish the identified regions as likely binding interfaces on TonB for its interaction with these periplasmic binding proteins. Sequence comparisons identifying conserved regions of secondary structure indicate the utility of assessing other class III periplasmic binding proteins for their interactions with TonB.

Our DLS data are consistent with conformational changes in both BtuF and TonB and with conformational changes in BtuF upon binding of cyanocobalamin. These outcomes support molecular dynamics simulations (*36*) that demonstrated a predominantly closed conformation for cyanocobalamin-bound BtuF compared to apo-BtuF. TonB−BtuF complexes had a R_H that was intermediate between that of TonB and of BtuF. These outcomes suggest that their complexation induces conformational change in TonB to a less elongated structure.

Interactions between TonB and BtuF were verified by our SPR and fluorescence experiments. SPR demonstrated an interaction that was specific and concentration-dependent, yet deviated from a simple binding model. The S-shaped binding isotherms (Figure 6C,D) and convex Scatchard transformations (insets in Figure 6C,D) are consistent with a more complex binding mechanism. Increases in tryptophan fluorescence generally signal a decrease in polarity of the environment of this residue. Trp174 was among the potential binding residues identified in region II, and Trp221 is proximal to potential binding residues in region III (Figures 3 and 5). In addition, Trp63 coordinates cyanocobalamin and is associated with a conserved α-helical

region within the N-terminal domain (Figure 5). Titration of TonB into BtuF augmented fluorescence emissions (Figure 7) while producing a blue shift in the BtuF emission spectrum. These observations are consistent with conformational change of these or nearby residues and also imply that conformational changes upon complexation suggested by our DLS data occurred not only in TonB but also in BtuF. S-shaped binding isotherms derived from our fluorescence assays, consistent with our SPR outcomes, also suggest a multifaceted interaction. Outcomes from fluorescence experiments were similar whether TonB or BtuF was the titrant. Taken together, our data indicate that TonB and BtuF interact with a 1:1 stoichiometry and that a coordinated binding mechanism describes engagement of the binding interfaces.

As with our TonB−FhuA and TonB−FhuD studies, concerns that uncleaved 6×His tags in our constructs might contribute to the observed TonB−BtuF interaction are unlikely for three main reasons. First, our phage display studies did not predict regions of interaction that included the 6×His tags. Second, 6×His tag-free TonB bound to immobilized 6×His-tagged FhuD in previous batch binding controls (unpublished data). Third, the His tags are net positive in our experimental buffers (pH 7.1−7.4), and their electrostatic repulsion would argue against their interaction.

Previously, TonB was demonstrated to interact with both apo- and substrate-bound OM receptor FhuA, but it bound to FhuA plus ferricrocin with much higher affinity (*3*), implying a sensing role for TonB in iron-deplete conditions. In contrast, discrimination between apo- and cyanocobalamin-bound BtuF by TonB (Figure 6) was not detected; this lack of discrimination was previously noted with FhuD and TonB (*21*).

We predicted TonB-binding residues within both lobes of BtuF. Regions I and II flank the binding cleft and include or are proximal to residues that bind cyanocobalamin. A TonB-binding interface within the siderophore binding cleft in FhuD was also predicted (*21*). Similarities in our phage display data for TonB−BtuF and TonB−FhuD interactions, in concert with outcomes from our biophysical experiments, suggest common features for the involvement of TonB at this stage of both transport cycles. This raises mechanistic questions about the temporal and spatial coordination of cyanocobalamin binding and TonB binding to BtuF. Cyanocobalamin and BtuF were reported to interact with a very high affinity of 15 nM (*12*). Our C_{50} values imply that TonB and BtuF may interact with comparatively lower affinity. Thus, cyanocobalamin could trigger displacement of TonB from its binding residues within the cleft of BtuF. Both fluorescence and SPR outcomes suggest that cyanocobalamin-bound BtuF binds TonB. Consequently, these data support our proposal that TonB does not engage all of its BtuF binding sites simultaneously.

Predicted binding residues span the length of the periplasmic region of TonB. The novel TonB−BtuF interactions that we have both identified and characterized can be integrated into what is already known about TonB-dependent transport while providing further insight into events in the periplasm. Data from this study are consistent with the previously proposed model (*21*) wherein TonB serves as a scaffold to promote efficient unidirectional transfer of substrate: binding of TonB to apo-BtuF may optimally position BtuF both to accept cyanocobalamin transported through the OM receptor BtuB and to deliver this substrate to the ABC transporter at the CM. Kadner and McElhaney (*37*) showed that TonB-mediated uptake of iron, an essential nutrient, occurs in preference to uptake of cyanocobalamin. For interaction of TonB with FhuD, apparent equilibrium dissociation constants between 20 nM and 310 nM were measured using SPR and extrinsic fluorescence (*21*). In contrast, the present study has produced C_{50} values for TonB−BtuF interaction of 0.5−0.6 μM. The disparity in the apparent affinity of TonB−BtuF versus TonB−FhuD interaction may reflect a physiologically motivated tendency where weaker affinity of TonB for BtuF allows TonB to give priority to its interaction with FhuD during iron-deplete conditions. We cannot reconcile the complex binding mechanism proposed for TonB−BtuF interactions versus the simple binding mechanism proposed for TonB−FhuD interactions. Differences in the nature and size of their cognate substrates may be important factors that determine mechanism.

Our phage display data predict that BtuF interacts with TonB residue Gln160, a residue whose interaction with OM protein BtuB has been demonstrated by cross-linking studies (*6*). Hence, although this prediction implies that a BtuB−TonB−BtuF triprotein complex may not be sterically feasible, formation of such a complex cannot be ruled out if BtuF binding sites on TonB are not all engaged simultaneously. Such temporally discriminate use of binding sites could also explain why common residues within regions I and III of BtuF (Figure 3) that have been shown to coordinate cyanocobalamin (*15*, *16*) are also now predicted to bind TonB. Similar quantitative outcomes for binding in the absence and presence of cyanocobalamin suggest that affinities for the different binding interfaces may be comparable. Whether, in performing its scaffolding function, TonB remains associated with BtuF or whether a binding−release−rebinding event occurs cannot be determined presently. Future studies will characterize interactions at each predicted binding interface on TonB and on BtuF.

BtuF can form a stable complex with BtuCD *in vitro* (*15*). It has been suggested that this association is retained throughout the transport cycle (*31*). It is difficult to reconcile this mechanism with our present study. However, given that BtuF may be present by as much as 50-fold excess of BtuC (*38*), apo-BtuF bound to BtuC may be exchanged for cyanocobalamin-bound BtuF. Rates of ATP hydrolysis measured in proteoliposomes maintained in nonionic detergents were shown to increase in the presence of cyanocobalamin (*31*). This argues for a preference for BtuC to engage cyanocobalamin-bound BtuF. Whether cyanocobalamin diffuses into an existing BtuF−BtuCD complex or whether apo- and cyanocobalamin-bound BtuF are exchanged merits further investigation. Our long-term goal is to identify the trigger that activates disengagement of cyanocobalamin-bound BtuF from TonB.

ACKNOWLEDGMENT

The authors thank C. Ng-Thow-Hing for bioinformatics and experimental support and D. M. Carter, J. C. Deme, H. Gagnon, S. G. Paquette, and A. M. Berghuis for technical support. We also thank S. Gruenheid, H. Le Moual, and R. E. MacKenzie for helpful discussions and J. A. Kashul for editorial support.

SUPPORTING INFORMATION AVAILABLE

Qualities of TonB and of BtuF purifications (Figure S1) and BtuF affinity-selected peptides that aligned to BtuC (Tables S1 and S2 and Figure S2). This material is available free of charge via the Internet at http://pubs.acs.org.

REFERENCES

1. Braun, V., Killmann, H., and Benz, R. (1994) Energy-coupled transport through the outer membrane of *Escherichia coli* small deletions in the gating loop convert the FhuA transport protein into a diffusion channel. *FEBS Lett. 346*, 59–64.
2. Peacock, R. S., Weljie, A. M., Peter, H. S., Price, F. D., and Vogel, H. J. (2005) The solution structure of the C-terminal domain of TonB and interaction studies with TonB box peptides. *J. Mol. Biol. 345*, 1185–1197.
3. Khursigara, C. M., De Crescenzo, G., Pawelek, P. D., and Coulton, J. W. (2004) Enhanced binding of TonB to a ligand-loaded outer membrane receptor: role of the oligomeric state of TonB in formation of a functional FhuA-TonB complex. *J. Biol. Chem. 279*, 7405–7412.
4. Kaserer, W. A., Jiang, X., Xiao, Q., Scott, D. C., Bauler, M., Copeland, D., Newton, S. M., and Klebba, P. E. (2008) Insight from TonB hybrid proteins into the mechanism of iron transport through the outer membrane. *J. Bacteriol. 190*, 4001–4016.
5. Ogierman, M., and Braun, V. (2003) Interactions between the outer membrane ferric citrate transporter FecA and TonB: studies of the FecA TonB box. *J. Bacteriol. 185*, 1870–1885.
6. Cadieux, N., and Kadner, R. J. (1999) Site-directed disulfide bonding reveals an interaction site between energy-coupling protein TonB and BtuB, the outer membrane cobalamin transporter. *Proc. Natl. Acad. Sci. U.S.A. 96*, 10673–10678.
7. Pawelek, P. D., Croteau, N., Ng-Thow-Hing, C., Khursigara, C. M., Moiseeva, N., Allaire, M., and Coulton, J. W. (2006) Structure of TonB in complex with FhuA, *E. coli* outer membrane receptor. *Science 312*, 1399–1402.
8. Shultis, D. D., Purdy, M. D., Banchs, C. N., and Wiener, M. C. (2006) Outer membrane active transport: structure of the BtuB:TonB complex. *Science 312*, 1396–1399.
9. Larsen, R. A., Thomas, M. G., and Postle, K. (1999) Protonmotive force, ExbB and ligand-bound FepA drive conformational changes in TonB. *Mol. Microbiol. 31*, 1809–1824.
10. Ghosh, J., and Postle, K. (2005) Disulphide trapping of an *in vivo* energy-dependent conformation of *Escherichia coli* TonB protein. *Mol. Microbiol. 55*, 276–288.
11. Braun, V. (2003) Iron uptake by *Escherichia coli*. *Front. Biosci. 8*, s1409–s1421.
12. Cadieux, N., Bradbeer, C., Reeger-Schneider, E., Koster, W., Mohanty, A. K., Wiener, M. C., and Kadner, R. J. (2002) Identification of the periplasmic cobalamin-binding protein BtuF of *Escherichia coli*. *J. Bacteriol. 184*, 706–717.
13. Hvorup, R. N., Goetz, B. A., Niederer, M., Hollenstein, K., Perozo, E., and Locher, K. P. (2007) Asymmetry in the structure of the ABC transporter-binding protein complex BtuCD-BtuF. *Science 317*, 1387–1390.
14. Braun, V., and Endriss, F. (2007) Energy-coupled outer membrane transport proteins and regulatory proteins. *Biometals 20*, 219–231.
15. Borths, E. L., Locher, K. P., Lee, A. T., and Rees, D. C. (2002) The structure of *Escherichia coli* BtuF and binding to its cognate ATP binding cassette transporter. *Proc. Natl. Acad. Sci. U.S.A. 99*, 16642–16647.
16. Karpowich, N. K., Huang, H. H., Smith, P. C., and Hunt, J. F. (2003) Crystal structures of the BtuF periplasmic-binding protein for vitamin B12 suggest a functionally important reduction in protein mobility upon ligand binding. *J. Biol. Chem. 278*, 8429–8434.
17. Clarke, T. E., Ku, S. Y., Dougan, D. R., Vogel, H. J., and Tari, L. W. (2000) The structure of the ferric siderophore binding protein FhuD complexed with gallichrome. *Nat. Struct. Biol. 7*, 287–291.
18. Ho, W. W., Li, H., Eakanunkul, S., Tong, Y., Wilks, A., Guo, M., and Poulos, T. L. (2007) Holo- and apo-bound structures of bacterial periplasmic heme-binding proteins. *J. Biol. Chem. 282*, 35796–35802.
19. Lawrence, M. C., Pilling, P. A., Epa, V. C., Berry, A. M., Ogunniyi, A. D., and Paton, J. C. (1998) The crystal structure of pneumococcal surface antigen PsaA reveals a metal-binding site and a novel structure for a putative ABC-type binding protein. *Structure 6*, 1553–1561.
20. Lee, Y. H., Deka, R. K., Norgard, M. V., Radolf, J. D., and Hasemann, C. A. (1999) *Treponema pallidum* TroA is a periplasmic zinc-binding protein with a helical backbone. *Nat. Struct. Biol. 6*, 628–633.
21. Carter, D. M., Miousse, I. R., Gagnon, J.-N., Martinez, E., Clements, A., Lee, J., Hancock, M. A., Gagnon, H., Pawelek, P. D., and Coulton, J. W. (2006) Interactions between TonB from *Escherichia coli* and the periplasmic protein FhuD. *J. Biol. Chem. 281*, 35413–35424.
22. Khursigara, C. M., De Crescenzo, G., Pawelek, P. D., and Coulton, J. W. (2005) Kinetic analyses reveal multiple steps in forming TonB-FhuA complexes from *Escherichia coli*. *Biochemistry 44*, 3441–3453.
23. Carter, D. M., Gagnon, J.-N., Damlaj, M., Mandava, S., Makowski, L., Rodi, D. J., Pawelek, P. D., and Coulton, J. W. (2006) Phage display reveals multiple contact sites between FhuA, an outer membrane receptor of *Escherichia coli*, and TonB. *J. Mol. Biol. 357*, 236–251.
24. James, K. J., Hancock, M. A., Moreau, V., Molina, F., and Coulton, J. W. (2008) TonB induces conformational changes in surface-exposed loops of FhuA, outer membrane receptor of *Escherichia coli*. *Protein Sci. 17*, 1679–1688.
25. Mandava, S., Makowski, L., Devarapalli, S., Uzubell, J., and Rodi, D. J. (2004) RELIC—a bioinformatics server for combinatorial peptide analysis and identification of protein-ligand interaction sites. *Proteomics 4*, 1439–1460.
26. Endriss, F., Braun, M., Killmann, H., and Braun, V. (2003) Mutant analysis of the *Escherichia coli* FhuA protein reveals sites of FhuA activity. *J. Bacteriol. 185*, 4683–4692.
27. Schuck, P. (2000) Size-distribution analysis of macromolecules by sedimentation velocity ultracentrifugation and lamm equation modeling. *Biophys. J. 78*, 1606–1619.
28. Laue, T. M., Shah, B. D., Ridgeway, T. M., and Pelletier, S. L. (1992) Computer-aided interpretation of analytical sedimentation data for proteins, in Analytical Ultracentrifugation in Biochemistry and Polymer Science (Harding, S., Rowe, A., and Horton, J., Eds.) pp 90−125, Royal Society of Chemistry, London.
29. Blondel, A., and Bedouelle, H. (1990) Export and purification of a cytoplasmic dimeric protein by fusion to the maltose-binding protein of *Escherichia coli*. *Eur. J. Biochem. 193*, 325–330.
30. Sangrar, W., Gabel, B. R., Boffa, M. B., Walker, J. B., Hancock, M. A., Marcovina, S. M., Horrevoets, A. J., Nesheim, M. E., and Koschinsky, M. L. (1997) The solution phase interaction between apolipoprotein(a) and plasminogen inhibits the binding of plasminogen to a plasmin-modified fibrinogen surface. *Biochemistry 36*, 10353–10363.
31. Borths, E. L., Poolman, B., Hvorup, R. N., Locher, K. P., and Rees, D. C. (2005) *In vitro* functional characterization of BtuCD-F, the *Escherichia coli* ABC transporter for vitamin B12 uptake. *Biochemistry 44*, 16301–16309.
32. Brewer, S., Tolley, M., Trayer, I. P., Barr, G. C., Dorman, C. J., Hannavy, K., Higgins, C. F., Evans, J. S., Levine, B. A., and Wormald, M. R. (1990) Structure and function of X-Pro dipeptide repeats in the TonB proteins of *Salmonella typhimurium* and *Escherichia coli*. *J. Mol. Biol. 216*, 883–895.
33. Kodding, J., Killig, F., Polzer, P., Howard, S. P., Diederichs, K., and Welte, W. (2005) Crystal structure of a 92-residue C-terminal fragment of TonB from *Escherichia coli* reveals significant conformational changes compared to structures of smaller TonB fragments. *J. Biol. Chem. 280*, 3022–3028.
34. Koedding, J., Howard, P., Kaufmann, L., Polzer, P., Lustig, A., and Welte, W. (2004) Dimerization of TonB is not essential for its binding to the outer membrane siderophore receptor FhuA of *Escherichia coli*. *J. Biol. Chem. 279*, 9978–9986.
35. Chang, C., Mooser, A., Pluckthun, A., and Wlodawer, A. (2001) Crystal structure of the dimeric C-terminal domain of TonB reveals a novel fold. *J. Biol. Chem. 276*, 27535–27540.
36. Kandt, C., Xu, Z., and Tieleman, D. P. (2006) Opening and closing motions in the periplasmic vitamin B12 binding protein BtuF. *Biochemistry 45*, 13284–13292.
37. Kadner, R. J., and McElhaney, G. (1978) Outer membrane-dependent transport systems in *Escherichia coli*: turnover of TonB function. *J. Bacteriol. 134*, 1020–1029.
38. Richarme, G., and Caldas, T. D. (1997) Chaperone properties of the bacterial periplasmic substrate-binding proteins. *J. Biol. Chem. 272*, 15607–15612.